
# Strathprints Institutional Repository

# Analysis of Stability and Convergence of Finite-Difference Methods for a Reaction-Diffusion problem on a One-Dimensional Growing Domain

by

J.A. Mackenzie* and A. Madzvamuse**

jam@maths.strath.ac.uk a.madzvamuse@sussex.ac.uk

Department of Mathematics *
University of Strathclyde
Livingstone Tower
26 Richmond Street
Glasgow, Scotland G1 1XH

Department of Mathematics **
University of Sussex
Mantell Building
Brighton
England, BN1 9RF

*Subject classification*: AMS(MOS) 65M06 65M12

*Keywords*: reaction-diffusion, growing domain, stability, bilogical pattern formation, exponential and logistic growth functions.

*Running Head*: Reaction-diffusion equations on growing domains.

*Mailing address*: Dr. J.A. Mackenzie

Department of Mathematics

University of Strathclyde

Livingstone Tower

26 Richmond Street

Glasgow, G1 1XH

Scotland

email: jam@maths.strath.ac.uk

fax: +44 (0)141 552 8657

*Abstract*

In this paper we consider the stability and convergence of finite difference discretisations of a reaction-diffusion equation on a one-dimensional domain which is growing in time. We consider discretisations of conservative and non-conservative formulations of the governing equation and highlight the different stability characteristics of each. Although non-conservative formulations are the most popular to date, we find that discretisations of the conservative formulation inherit greater stability properties. Furthermore, we present a novel adaptive time integration scheme based on the well-known $\theta$-method and describe how the parameter $\theta$ should be chosen to ensure unconditional stability, independently of the rate of domain growth. This work is a preliminary step towards an analysis of numerical schemes for the solution of reaction-diffusion systems on growing domains. Such problems arise in many practical areas including biological pattern formation and tumour growth.

# 1 Introduction

In his seminal paper Turing [24] considered a system of two reacting and diffusing chemicals (which he termed *morphogens*) and demonstrated the surprising phenomenon of diffusion-driven instability. That is, he showed that it was possible for a spatially uniform steady state, linearly stable in the absence of diffusion, to be driven unstable by the presence of diffusion and evolve to a spatially non-uniform steady state. Turing patterns were first observed by Castets *et al* [2] in a chloride-ionic-malonic-acid (CIMA) reaction and Ouyang and Swinney [20] were the first to observe Turing instability from a spatially uniform state to a patterned state. Although controversial for many years, recent experimental findings strongly support this as a mechanism for the formation of repeated structures in skin organ formation [18, 22] and zebrafish mesoderm cell fates [23].

Most of the applications of Turing theory have assumed fixed domains. For example, in the context of developmental biology, the tacit assumption is that pattern forming processes occur on a much faster timescale in comparison to domain growth. However, it has been shown that in some cases this is not true and that domain growth and domain shape can play a very important role in pattern formation and selection. For example, Kondo and Asai [9] illustrated the role of domain growth in pattern formation by finding mode doubling in patterns of the angelfish *Pomacanthus* as it grows. The juvenile *Pomacanthus* has three vertical stripes; once the fish grows to twice its length, new stripes emerge between the original stripes so that the original wavelength is maintained.

The nonlinear nature of the governing equations, coupled with domain growth, means that obtaining meaningful analytical solutions is not feasible and that efficient, accurate and robust numerical simulations are required. On regular fixed domains the most widely used numerical method to solve reaction-diffusion equations (RDEs) is the centred finite difference scheme. Its popularity stems from its simplicity and ability to handle boundary conditions in a straightfor-

ward way [3, 9, 21]. On the other hand, the application of finite difference methods to complicated, irregular, and sometimes continuously growing domains is not trivial. It is well known that finite element methods can be applied easily to complicated domains and continuously changing boundaries can be handled readily by moving grid finite element methods (MGFEM). Madzvamuse *et al* [14, 15, 16] investigated, through a novel application of the MGFEM, the role of domain growth to pattern generation on both regular and irregular domains. Numerical simulations in one dimension show solution behaviours such as mode- and period-doubling, peak insertion and splitting. In two dimensions a variety of bifurcations are observed such as transitions from stripe-to-stripe patterns, spots-to-stripes-to-spots patterns, circular patterns and period doubling of spots-patterns.

It can be shown that a reaction-diffusion system on a growing domain can be transformed into a reaction-diffusion system on a fixed domain, but with time-dependence in the diffusion and dilution terms [21]. Since growing domains effectively change diffusion rates, the mathematical and numerical understanding of the effects of growth on Turing patterns is an important problem. To solve a problem posed on a moving domain it is common to use a reformulation using an alternative frame of reference rather than the standard fixed Eulerian frame. For fluid dynamics problems one could decide to use a Lagrangian transformation to follow the fluid flow. More generally however, there may be no obvious or preferred reference frame, and if the domain moves in time one may simply be satisfied with a transformation from a fixed stationary domain $\Omega_c$ onto the physically evolving domain $\Omega_t$. The Arbitrary Lagrangian Eulerian (ALE) formulation was introduced for this purpose and it has been used successfully to tackle a number of physical applications such as fluid-structure interaction systems (see [5, 8]). Originally ALE numerical schemes were mainly based on finite difference (ALE-FD) or finite volume methods (ALE-FV) as the application areas were compressible flow problems such as aeroelastics [10]. More recently, ALE methods have been developed within a finite element framework (ALE-FEM) [1, 6, 7] and applied to fluid-structure

interaction problems in haemodynamics [19].

Formaggia and Nobile [7] discuss a number of issues related to the formulation of weak ALE formulations for a model scalar convection-diffusion equation; these include the spatial discretisation by Galerkin finite element methods, and the stability of schemes for the numerical integration in time of the resulting semi-discrete approximations. An interesting and unexpected outcome of their analysis is the observation that certain implicit temporal integration schemes are only *conditionally stable* depending on the movement of the computational mesh, whereas the same schemes are *unconditionally stable* when applied to problems posed on fixed meshes. In an attempt to construct an unconditionally stable second-order time integration method, in [11] an analysis was performed of various time integration schemes for a FD-ALE discretisation of a one-dimensional model convection-diffusion problem. By carefully accounting for the diffusive and anti-diffusive effects of the discretisation of the additional terms in the governing equation, the authors were able to propose an adaptive $\theta$-method time integrator which is unconditionally stable, irrespective of the movement of the mesh and is asymptotically second-order accurate in time if the mesh evolves smoothly. It was recently established that with suitable modifications, the same time integrator can successfully be applied to construct an unconditionally stable second-order time integration scheme for a ALE-FEM discretisation of a two-dimensional convection-diffusion problem [12].

It is well known that for Turing instabilities to arise it is necessary to have a difference in the diffusivities of the two chemically reacting species [24]. Fully discrete numerical approximations of Turing systems on growing domains are likely to give rise to additional numerical dissipation and hence it is important to determine if this artificial dissipation affects the biological pattern formation process. The precise identification of numerical dissipation was essential in the stability analysis of Mackenzie and Mekwi [11, 12]. The analysis presented in [7, 11, 12] addresses the problem of convection and diffusion of a scalar quantity through a medium that is stationary,

although the overall domain may vary with time due to the movement of the domain boundary. For biological growth problems however, it is natural to assume that diffusion and reactions occur in a medium that is moving according to some growth protocol. We will see that when a domain grows it gives rise to an additional convection-like term which is not divergence free. This additional term has a diluting effect on the growth of the analytical solution but we will see that this qualitative behaviour can often be lost under discretisation.

Despite the recent interest in convection-diffusion problems on moving domains, to our knowledge very little analysis has been performed for RDEs on continuously deforming domains, where domain growth occurs through a prescribed growth function or can be modelled from experiments as is the case in biology and bio-medicine [17]. The need for such an analysis is evident from the numerical experiments presented in [14], where it was found that domain growth greatly influenced the selection of symmetric solutions obtained using finite difference discretisations.

The layout of this paper is as follows: In Section 2 we present a model reaction-diffusion equation which has been modified to include domain growth. In this section we also consider conservative and non-conservative reformulations of the governing equation with respect to a time independent reference frame. We also derive an energy estimate for the growth of the solution in the special case of linear reaction kinetics and an exponentially growing domain. In Section 3 we present the finite difference spatial discretisations of the conservative and non-conservative formulations. In Section 4 we analyse the stability properties of four fully discrete approximations for the model problem of linear reaction on a uniformly growing domain. Conservative discretisations of a linear reaction-diffusion equation are considered in Section 5, where we also present a novel adaptive $\theta$-method and show it is unconditional stable. We prove convergence of the adaptive $\theta$-method in Section 6 and present some numerical experiments in Section 7. Finally, we draw some conclusions and outline some areas for further research in Section 8.

# 2 Model Problem

Reaction-diffusion systems of the type studied in pattern formation generally exclude cross-diffusion, and are only coupled by the reaction kinetics terms. Therefore, we can consider the behaviour of a single chemical species with a straightforward generalisation to a system of interacting chemicals. Let $T > 0$ and for each $t \in [0, T]$, $\Omega_t$ be a bounded domain in $\mathbb{R}$. We shall use the notation

$$Q_T = \{(x, t) \in \mathbb{R}^2 : \ x \in \Omega_t, \ t \in (0, T)\}.$$

Growth of the domain $x \in \Omega_t$ with boundary $\partial\Omega_t$ generates a flow $a(x, t)$. Application of Reynolds transport theorem to the equation for mass conservation for a chemical $C$, which diffuses with constant density diffusivity $\kappa$, undergoing reaction at rate $\gamma f(c)$, gives (see [3])

$$\left.\begin{aligned} \frac{\partial c}{\partial t} + \frac{\partial}{\partial x}\left(ac - \kappa\frac{\partial c}{\partial x}\right) + \gamma f(c) = 0, \qquad (x, t) \in Q_T \\ c = c_0(x), \quad x \in \Omega_0, \ t = 0 \\ c = 0, \quad x \in \partial\Omega_t, \ t > 0, \end{aligned}\right\} \tag{2.1}$$

where $c(x, t)$ is the concentration at position $x$ at time $t$ and $c_0(x)$ is a well-defined positive bounded function. The time-varying domain introduces two new terms to the standard reaction-diffusion equation: $ac_x$, the transport of material around the domain and $ca_x$, the diluting (concentrating) effect of the local volume increase (decrease).

## 2.1 Arbitrary Lagrangian-Eulerian (ALE) Transformation

When the domain is growing a common frame of reference adopted for numerical approximations is the Arbitrary Lagrangian Eulerian (ALE) frame. Let $\mathcal{A}_t$ be a family of mappings, which at each $t \in [0, T]$ maps the points $\xi$ of a reference or computational domain $\Omega_c$, into the points of the

domain $\Omega_t$ at time $t$, so that

$$\mathcal{A}_t : \quad \Omega_c \in \mathbb{R} \to \Omega_t \in \mathbb{R}, \quad x(\xi, t) = \mathcal{A}_t(\xi).$$

We assume that $\mathcal{A}_t$ is bijective and $\Omega_t = \mathcal{A}_t(\Omega_c)$ is bounded. We also assume $\mathcal{A}_t$ and its inverse $\mathcal{A}_t^{-1}$ are sufficiently smooth. For a function $g : Q_T \to \mathbb{R}$ defined on the physical domain, the time derivative with respect to the fixed reference domain is

$$\dot{g} \equiv \left.\frac{\partial g}{\partial t}\right|_{\xi} : \quad Q_T \to \mathbb{R}.$$

If $c : \ Q_T \to \mathbb{R}$ is regular enough, then by the chain rule

$$\dot{c} = \left.\frac{\partial c}{\partial t}\right|_{x} + \dot{x} \left.\frac{\partial c}{\partial x}\right|_{x}.$$

The ALE mapping $\mathcal{A}_t$ generates a velocity $\dot{x}$ defined as

$$\dot{x}(x, t) = \left.\frac{\partial x}{\partial t}\right|_{\xi} (\mathcal{A}_t^{-1}(x), t).$$

Rewriting the governing equation (2.1) with respect to the fixed computational coordinates we have

$$\dot{c} - \kappa \frac{\partial c}{\partial x^2} - (\dot{x} - a)\frac{\partial c}{\partial x} + c\frac{\partial a}{\partial x} + \gamma f(c) = 0, \quad (x, t) \in Q_T.$$

If the mapping onto the computational domain is chosen such that $\dot{x} = a$, then the transformation is purely Lagrangian and we arrive at the reaction-diffusion equation

$$\dot{c} - \kappa \frac{\partial^2 c}{\partial x^2} + c\frac{\partial a}{\partial x} + \gamma f(c) = 0 \quad (x, t) \in Q_T. \tag{2.2}$$

Before we discuss numerical approximations of our model problem we first consider the effect that domain growth has on the behaviour of the solution.

## 2.2 Basic energy estimate

In this section we derive a basic energy estimate for the growth of the $L_2$ norm of the solution of (2.2), where to simply the presentation we will assume linear reaction kinetics $f(c) = c$ and a

uniform growth of the domain so that $a_x > 0$ is a constant. Note that $a_x$ is constant if and only domain growth is exponential [13]

**Theorem 2.1** *The solution of (2.2) with $a_x$ constant and $f(c) = c$ satisfies the following bound*

$$||c||^2_{L_2(\Omega_t)} + 2\kappa \int_0^t e^{-(a_x+2\gamma)(t-s)} ||c_x||^2_{L_2(\Omega_s)} \, \mathrm{d}s = e^{-(a_x+2\gamma)t} ||c_0||^2_{L_2(\Omega_0)}. \tag{2.3}$$

**Proof** Multiplying (2.2) by $c$ and integrating over $\Omega_t$ we have

$$\int_{\Omega(t)} c\,\dot{c}\,\mathrm{d}x + \kappa \int_{\Omega_t} c_x^2 \,\mathrm{d}x + (a_x + \gamma) \int_{\Omega_t} c^2 \,\mathrm{d}x = 0,$$

where we have used integration by parts and the boundary conditions on $c$ to simplify the diffusion term. Using Reynolds transport theorem we have

$$\begin{aligned} \int_{\Omega_t} c\,\dot{c}\,\mathrm{d}x &= \int_{\Omega_t} \frac{1}{2}\frac{d}{dt}(c^2)\,\mathrm{d}x \\ &= \frac{1}{2}\left[\frac{d}{dt}\int_{\Omega_t} c^2\,\mathrm{d}x - \int_{\Omega_t} a_x c^2\,\mathrm{d}x\right]. \end{aligned}$$

Therefore, we arrive at the differential equality

$$\frac{d}{dt}||c||^2_{L_2(\Omega_t)} + 2\kappa||c_x||^2_{L_2(\Omega_t)} + (a_x + 2\gamma)||c||^2_{L_2(\Omega_t)} = 0$$

and the final result follows from a standard Grönwall argument. □

From (2.3) we can see that domain growth has a diluting effect on the $L_2$ norm of the solution. In particular, we can see that, if $a_x + 2\gamma > 0$, then $||c||_{L_2(\Omega_t)} \to 0$ as $t \to \infty$. In what follows it will become clear that replicating this qualitative behaviour of numerical approximations is non-trivial.

## 2.3 Uniform domain growth

The second derivative appearing in (2.2) can be rewritten in terms of the derivatives with respect to computational coordinates and we find that

$$\dot{c} - \kappa\left(\frac{c_{\xi\xi}}{x_\xi^2} - \frac{x_{\xi\xi}}{x_\xi}c_\xi\right) + a_x c + \gamma f(c) = 0, \quad (\xi, t) \in \Omega_c \times [0, T]. \tag{2.4}$$

To make further headway we will assume that the domain growth is uniform and isotropic so that

$$x(\xi,t) = \rho(t)\,\xi, \quad \text{where} \quad \rho(0) = 1,\ \rho(t) > 0, \quad \forall\, t > 0, \tag{2.5}$$

with $x \in \Omega_t$, $\xi \in \Omega_c$, and $\rho(t)$ is the growth function. If $\dot{x} = a$, then it is easy to show that $a_x = \dot{\rho}(t)/\rho(t)$ and in this case (2.4) simplifies to

$$\dot{c} - \frac{\kappa}{\rho^2(t)} c_{\xi\xi} + a_x c + \gamma f(c) = 0. \tag{2.6}$$

The coordinate transformation (2.5) therefore results in a reaction-diffusion equation with a time-dependent diffusion coefficient.

We will also be interested in an alternative conservative formulation

$$(\dot{\rho c}) - \kappa \left( \frac{c_\xi}{\rho} \right)_\xi + \rho\gamma f(c) = 0, \tag{2.7}$$

which can be obtained by multiplying (2.6) by $\rho$ and using the fact that $a_x = \dot{\rho}/\rho$. The non-conservative and the conservative formulation are equivalent at the continuous level but we will see that their numerical discretisations inherit different stability properties.

# 3 Moving mesh discretisations

We consider semi-discretisations of (2.6) and (2.7) using second-order central finite difference approximations of the spatial derivatives of $c$. We will assume that the domain $\Omega_t = [x_l(t), x_r(t)]$ is covered by a mesh of $N$ cells with

$$x_l(t) = x_0(t) < x_1(t) < \ldots < x_{N-1}(t) < x_N(t) = x_r(t).$$

The moving mesh in physical space is assumed to be the image of a fixed uniform mesh covering the computational domain $\Omega_c = [0, 1]$, via the mapping $x(\xi, t)$, so that

$$x_j(t) = x(\xi_j, t) = x(j/N, t), \quad j = 0, \ldots, N.$$

The measure of each physical cell will be denoted by

$$h_j(t) = x_j(t) - x_{j-1}(t), \quad j = 1, \ldots, N.$$

When we have uniform growth (2.5) then

$$h_j(t) = \rho(t)\Delta\xi = \frac{\rho(t)}{N}, \quad j = 1, \ldots, N.$$

To define the semi-discretisations we will use the notation $c_j^n$ to denote the approximation of $c(x_j^n, t^n)$ and $\boldsymbol{c}^n = (c_0^n, c_1^n, \ldots, c_{N-1}^n, c_N^n)^T$. We will use the forward and backward divided differences

$$(D_+\boldsymbol{c})_j = \frac{c_{j+1} - c_j}{h_{j+1}} \qquad \text{and} \qquad (D_-\boldsymbol{c})_j = \frac{c_j - c_{j-1}}{h_j}.$$

Using this notation the semi-discretisations of (2.6) and (2.7) take the form

$$\dot{c}_j = \frac{1}{\Delta\xi}\left(\frac{\kappa}{\rho}(D_+ - D_-)\boldsymbol{c}\right)_j - a_x c_j - \gamma f(c_j) \tag{3.1}$$

and

$$(\dot{\rho c})_j \;=\; \frac{1}{\Delta\xi}\left(\kappa(D_+ - D_-)\boldsymbol{c}\right)_j - \gamma\rho f(c_j)\,. \tag{3.2}$$

In the following subsections we consider various temporal discretisations of (3.1) and (3.2) and the stability of the resulting fully discrete schemes. The analysis will be carried out using the following mesh-dependent norms. For the numerical solution we use the $L_2$ norm (noting the homogeneous boundary conditions)

$$||\boldsymbol{c}||_n = \left(\sum_{j=1}^{N-1}\left(\frac{h_{j+1}^n + h_j^n}{2}\right)(c_j)^2\right)^{\frac{1}{2}}.$$

Approximations of the derivatives will be measured in the cell-based norm

$$||\boldsymbol{v}||_{\overline{n}} = \left(\sum_{j=1}^{N} h_j^n (v_j)^2\right)^{\frac{1}{2}}.$$

In the following sections we will consider the different stability characteristics of temporal discretisations of the semi-discretisations (3.1) and (3.2).

# 4 Stability analysis for linear reaction on an exponentially growing domain

To get some idea of the effect of the growth of the domain on the stability of fully discrete approximations of the conservative and non-conservative formulations, we initially consider the simplified model problem with $\kappa = 0$, $f(c) = c$, with $\gamma$ a positive constant. Furthermore, we will assume that we have uniform isotropic exponential growth so $x(t) = \xi e^{St}$, $S > 0$, and hence $\rho(t) = e^{St}$ and $a_x = S$.

## 4.1 Backward-Euler applied to conservative formulation

Discretising (3.2) in time using the first-order backward Euler (BE) scheme we get

$$\frac{\rho^{n+1}c_j^{n+1} - \rho^n c_j^n}{\Delta t} = -\gamma \rho^{n+1} c_j^{n+1}. \tag{4.1}$$

Rearranging (4.1) we get

$$\begin{aligned} c_j^{n+1} &= \frac{\rho^n}{\rho^{n+1}(1+\gamma\Delta t)} c_j^n \\ &= \frac{e^{-S\Delta t}}{(1+\gamma\Delta t)} c_j^n. \end{aligned} \tag{4.2}$$

It is clear from the above that the scheme is unconditionally stable with respect to the $l_\infty$ norm. Note that the effect of the growth of the domain on the dilution of the solution is captured **exactly** by the $e^{-S\Delta t}$ factor. However, as expected, the backward Euler treatment of the linear reaction term leads to an underestimation in the decrease in the solution as

$$\frac{1}{(1+\gamma\Delta t)} > e^{-\gamma\Delta t}.$$

If $\gamma \gg S$, then the first-order error due to the BE treatment of the reaction term is likely to pollute the accuracy of the solution even though no error arises from the treatment of the moving

domain. The analysis above can be extended to consider the behaviour of the numerical solution when measured in the mesh dependent $L_2$ norm. It is straightforward to establish from (4.2) that

$$||\boldsymbol{c}^{n+1}||_{n+1} = \frac{e^{-\frac{S\Delta t}{2}}}{(1+\gamma\Delta t)}||\boldsymbol{c}^{n}||_{n}. \tag{4.3}$$

Again, the scheme is unconditionally stable with respect to this norm.

## 4.2 Backward-Euler applied to non-conservative formulation

Discretising the non-conservative formulation (3.1) in time using the first-order backward Euler scheme we get

$$\frac{c_j^{n+1} - c_j^n}{\Delta t} = -(S+\gamma)c_j^{n+1}. \tag{4.4}$$

Rearranging (4.4) we get

$$c_j^{n+1} = \frac{1}{\big(1+(S+\gamma)\Delta t\big)}c_j^n.$$

Therefore, again the scheme is unconditionally stable with respect to the $l_\infty$ norm. This time an error is committed due to the growth of the domain as

$$\frac{1}{(1+\big(S+\gamma)\Delta t\big)} > e^{-(S+\gamma)\Delta t}.$$

Furthermore, the non-conservative scheme is less accurate than the conservative BE scheme as

$$\frac{1}{\big(1+(S+\gamma)\Delta t\big)} > \frac{e^{-S\Delta t}}{(1+\gamma\Delta t)} > e^{-(S+\gamma)\Delta t}.$$

The difference between the performance of both methods will be slight if $\gamma \gg S$ for the reasons mentioned above. However, when domain growth is fast compared to the reaction kinetics then $S \gg \gamma$ and the non-conservative method should be considerably less accurate than the conservative method. This will be verified by a numerical experiment at the end of this section. For the non-conservative formulation, in terms of the $L_2$ norm we can show that

$$||\boldsymbol{c}^{n+1}||_{n+1} = \frac{e^{\frac{S\Delta t}{2}}}{\big(1+(S+\gamma)\Delta t\big)}||\boldsymbol{c}^{n}||_{n}. \tag{4.5}$$

From (4.5) we can deduce that the BE scheme applied to the non-conservative formulation is only conditionally stable if $\Delta t < \Delta t^*$, where $\Delta t^*$ is the positive root of the nonlinear algebraic equation

$$e^{\frac{S\Delta t^*}{2}} - (S+\gamma)\Delta t^* - 1 = 0.$$

This result is somewhat surprising given that the method is fully implicit with respect to the reaction kinetics and is stable with respect to the $l_\infty$ norm. This can be explained by the fact that the $L_2$ norm depends on the measure of $\Omega_t$, whereas the $l_\infty$ norm does not. Therefore, what is actually happening is although the nodal value of $c_j^n$ are decreasing as $n \to \infty$, the rate of decrease is not fast enough to ensure that $||\boldsymbol{c}^n||_n \to 0$.

## 4.3 Crank-Nicolson applied to conservative formulation

Discretising (3.2) in time using the second-order Crank-Nicolson scheme we get

$$\frac{\rho^{n+1}c_j^{n+1} - \rho^n c_j^n}{\Delta t} = -\frac{\gamma}{2}(\rho^{n+1}c_j^{n+1} + \rho^n c_j^n).$$

As before we find that

$$c_j^{n+1} = e^{-S\Delta t}\left(\frac{1-\frac{\gamma\Delta t}{2}}{1+\frac{\gamma\Delta t}{2}}\right)c_j^n.$$

We get perfect dilution from the growth of the domain and the usual second-order Padé approximation of the negative exponential decrease from the linear reaction term. Clearly, the scheme is unconditionally stable in $l_\infty$. In terms of the $L_2$ norm we easily can show that

$$||\boldsymbol{c}^{n+1}||_{n+1} = e^{-\frac{S\Delta t}{2}}\left(\frac{1-\frac{\gamma\Delta t}{2}}{1+\frac{\gamma\Delta t}{2}}\right)||\boldsymbol{c}^n||_n,$$

and hence the method is unconditionally stable. We expect there to be quite a difference in the quality of the solutions between the BE and CN schemes due to the additional accuracy of the CN treatment of the reaction term. The difference will become less noticeable as $\gamma$ reduces in comparison to $S$.

## 4.4 Crank-Nicolson applied to non-conservative formulation

Discretising (3.1) in time using the second-order Crank-Nicolson scheme we get

$$\frac{c_j^{n+1} - c_j^n}{\Delta t} = -\frac{(S+\gamma)}{2}(c_j^{n+1} + c_j^n).$$

As before we find that

$$c_j^{n+1} = \left( \frac{1 - \frac{(S+\gamma)\Delta t}{2}}{1 + \frac{(S+\gamma)\Delta t}{2}} \right) c_j^n.$$

Again the scheme is unconditionally stable with respect to the $l_\infty$ norm and is second-order accurate. When $\gamma \gg S$ we expect there to be little difference in the quality of the solutions between the conservative and non-conservative CN schemes. The difference will increase however as $\gamma$ reduces in comparison to $S$. In terms of the $L_2$ norm we easily can show that

$$||\boldsymbol{c}^{n+1}||_{n+1} = e^{\frac{S\Delta t}{2}} \left| \frac{1 - \frac{(S+\gamma)\Delta t}{2}}{1 + \frac{(S+\gamma)\Delta t}{2}} \right| ||\boldsymbol{c}^n||_n.$$

As with the BE method applied to the non-conservative formulation, we find that the CN method is not unconditionally stable in the $L_2$ norm. In fact, the method is unstable for $\Delta t > \Delta t^*$, where $\Delta t^*$ is the solution of the nonlinear algebraic equation

$$e^{\frac{S\Delta t^*}{2}} \left| 1 - \left( \frac{S+\gamma}{2} \right) \Delta t^* \right| - \left( \frac{S+\gamma}{2} \right) \Delta t^* - 1 = 0.$$

Again this result shows that the discretisations of the non-conservative formulation are less stable than their equivalent discretisation of the conservative counterpart.

Figure 1 (a) shows the behaviour of $||\boldsymbol{c}^n||_n$ using the four methods given above. The calculations were performed using the parameters $\gamma = 1$, $S = 3$ and $\Delta t = 1$. Therefore, this experiment corresponds to a situation were domain growth dominates the decay of the solution due to the reaction kinetics. We can see clearly that the two discretisations of the conservative formulation significantly outperform the non-conservative discretisations. In fact, we can see that the solution obtained using the non-conservative CN scheme is increasing exponentially when measured in the

$L_2$ norm. We can also see that the non-conservative BE scheme is less accurate than the two conservative methods. Figure 1 (b) shows the results with $\gamma$ and $\Delta t$ as above, but this time we let $S = 0.5$. As expected, there is less discrepancy between the solutions but it is still true that the solutions obtained using the conservative formulations are considerably more accurate than those obtained using the non-conservative form.

The above analysis and results clearly demonstrate that when domain growth is very fast as compared to the reaction times, then non-conservation formulations are unreliable and should not be used. However, for slow growth, such formulations can be used.

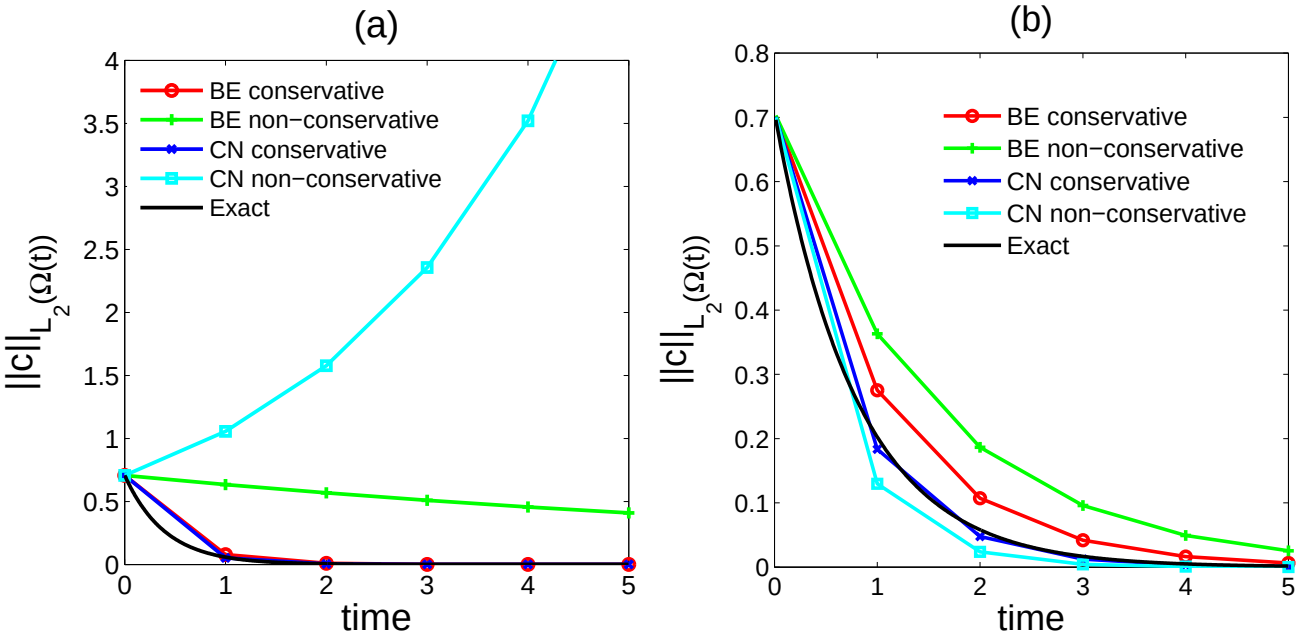


Figure 1: Evolution of $||\boldsymbol{c}^n||_n$ for linear reaction problem on an exponentially growing domain: (a) $S = 3$, $\gamma = 1$, $\Delta t = 1$ and (b) $S = 0.5$, $\gamma = 1$, $\Delta t = 1$.

# 5 Analysis of conservative methods for reaction-diffusion equation

The analysis in the previous section would appear to suggest that the methods based on the conservative formulation are inherently more stable and more accurate. In this section we will therefore concentrate on these methods and next examine the situation where $\kappa \neq 0$, $f(c) = c$ and we will again assume we have uniform growth of the domain.

## 5.1 Backward Euler

Discretising (3.2) using a backward Euler (BE) temporal discretisation and assuming $t_{n+1} - t_n = \Delta t$ yields the fully discrete scheme

$$(\rho c)_j^{n+1} = (\rho c)_j^n + \frac{\Delta t}{\Delta \xi}(\kappa(D_+ - D_-)\boldsymbol{c})_j^{n+1} - \gamma \Delta t (\rho c)_j^{n+1}\,. \tag{5.1}$$

For this scheme we have the following stability result.

**Theorem 5.1** *If the scheme (5.1) is applied to the conservative formulation (2.7), then*

$$||\boldsymbol{c}^{n+1}||_{n+1}^2 = (1+2\gamma\Delta t)^{-1}\left(||\boldsymbol{c}^n||_n^2 - ||\boldsymbol{c}^{n+1} - \boldsymbol{c}^n||_n^2 - 2\kappa\Delta t\,||D_+\boldsymbol{c}^{n+1}||_{\overline{n+1}}^2 - \Delta\xi\sum_{j=1}^{N-1}[\rho^{n+1} - \rho^n](c_j^{n+1})^2\right).$$

**Proof** Multiplying (5.1) by $c_j^{n+1}$ and summing over all interior nodes (since $c_0 = c_N = 0$), we have

$$\sum_{j=1}^{N-1} \rho^{n+1}(1 + \gamma\Delta t)(c_j^{n+1})^2 = \mathrm{I} + \mathrm{II},$$

where

$$\mathrm{I} = \sum_{j=1}^{N-1} \rho^n c_j^n c_j^{n+1}\,,$$

$$\mathrm{II} = \frac{\kappa\Delta t}{\Delta\xi}\sum_{j=1}^{N-1}\left[\left((D_+ - D_-)\boldsymbol{c}\right)_j^{n+1}\right]c_j^{n+1}.$$

Applying the identity

$$ab = \frac{1}{2}a^2 + \frac{1}{2}b^2 - \frac{1}{2}(a-b)^2 \tag{5.2}$$

to the product $c_j^n c_j^{n+1}$ in term I, we have

$$\begin{aligned} \mathrm{I} &= \frac{1}{2}\sum_{j=1}^{N-1}\rho^n\left[(c_j^n)^2 + (c_j^{n+1})^2 - (c_j^n - c_j^{n+1})^2\right] \\ &= \frac{1}{2\Delta\xi}\left(||\boldsymbol{c}^n||_n^2 + ||\boldsymbol{c}^{n+1}||_{n+1}^2 - ||\boldsymbol{c}^{n+1} - \boldsymbol{c}^n||_n^2\right) - \frac{1}{2}\sum_{j=1}^{N-1}[\rho^{n+1} - \rho^n](c_j^{n+1})^2. \end{aligned}$$

For the term II, we have

$$\begin{aligned} \mathrm{II} &= \frac{\kappa\Delta t}{\Delta\xi}\left[\sum_{j=1}^{N-1}\left(\frac{c_{j+1}^{n+1} - c_j^{n+1}}{h_{j+1}^{n+1}}\right)c_j^{n+1} - \sum_{j=0}^{N-2}\left(\frac{c_{j+1}^{n+1} - c_j^{n+1}}{h_{j+1}^{n+1}}\right)c_{j+1}^{n+1}\right] \\ &= -\frac{\kappa\Delta t}{\Delta\xi}\sum_{j=0}^{N-1}\left(\frac{c_{j+1}^{n+1} - c_j^{n+1}}{h_{j+1}^{n+1}}\right)^2 h_{j+1}^{n+1} = -\frac{\kappa\Delta t}{\Delta\xi}||D_+\boldsymbol{c}^{n+1}||_{\overline{n+1}}^2. \end{aligned}$$

Therefore, we have

$$||\boldsymbol{c}^{n+1}||_{n+1}^2 = (1+2\gamma\Delta t)^{-1}\left(||\boldsymbol{c}^n||_n^2 - ||\boldsymbol{c}^{n+1} - \boldsymbol{c}^n||_n^2 - 2\kappa\Delta t\,||D_+\boldsymbol{c}^{n+1}||_{\overline{n+1}}^2 - \Delta\xi\sum_{j=1}^{N-1}[\rho^{n+1} - \rho^n](c_j^{n+1})^2\right),$$

and this completes the proof. □

**Remark 1** *We note here the additional so-called numerical diffusion on the right-hand side of (5.1), which is represented by the term* $-||\boldsymbol{c}^{n+1} - \boldsymbol{c}^n||_n^2$. *Note that this term would not appear if the domain were stationary.*

**Remark 2** *This result shows that the discrete* $L_2$ *norm decreases independently of the time step as domain growth ensures that* $\rho^{n+1} - \rho^n > 0$.

## 5.2 Forward Euler

It is instructive to consider the forward Euler (FE) scheme for (3.2) which takes the form

$$(\rho c)_j^{n+1} = (\rho c)_j^n + \frac{\Delta t}{\Delta\xi}\big(\kappa(D_+ - D_-)\boldsymbol{c}\big)_j^n - \gamma\Delta t(\rho c)_j^n. \tag{5.3}$$

Multiplying (5.3) by $c_j^n$ and following the same analysis as for the BE discretisation, we find that

$$||\boldsymbol{c}^{n+1}||_{n+1}^2 = (1-2\gamma\Delta t)||\boldsymbol{c}^n||_n^2 + ||\boldsymbol{c}^{n+1}-\boldsymbol{c}^n||_{n+1}^2 - 2\kappa\Delta t||D_+\boldsymbol{c}^n||_{\overline{n}}^2 - \Delta\xi\sum_{j=1}^{N-1}[\rho^{n+1}-\rho^n](c_j^n)^2.$$

We now have an anti-diffusive term on the right-hand side caused by the mesh movement

$$||\boldsymbol{c}^{n+1}-\boldsymbol{c}^n||_{n+1}^2,$$

and hence the scheme will be conditionally stable on a moving mesh.

## 5.3 Mesh-dependent $\theta$-method

The question arises if it is possible to combine the BE and FE schemes to create a method that is unconditionally stable and second-order accurate in time. To push through the analysis we consider a weighted combination of a slight variation to the FE and BE schemes given earlier. The new method will involve the modified BE scheme

$$(\rho c)_j^{n+1} = (\rho c)_j^n + \frac{\Delta t}{\Delta\xi}\kappa\left(\frac{c_{j+1}^{n+1}-c_j^{n+1}}{h_{j+1}^\theta} - \frac{c_j^{n+1}-c_{j-1}^{n+1}}{h_j^\theta}\right) - \gamma\Delta t(\rho c)_j^{n+1}, \tag{5.4}$$

where $h_j^\theta = \theta h_j^{n+1} + (1-\theta)h_j^n$. Note that the only difference between (5.1) and (5.4) is the value of $h_j$ used in the diffusive terms. Similarly, we use the modified FE scheme

$$(\rho c)_j^{n+1} = (\rho c)_j^n + \frac{\Delta t}{\Delta\xi}\kappa\left(\frac{c_{j+1}^{n}-c_j^{n}}{h_{j+1}^\theta} - \frac{c_j^{n}-c_{j-1}^{n}}{h_j^\theta}\right) - \gamma\Delta t(\rho c)_j^{n}. \tag{5.5}$$

Let us consider a weighted combination of the modified BE and FE schemes of the form $\theta(5.4) + (1-\theta)(5.5)$, with $\theta \in [0,1]$. The stability analysis will be carried out using the mesh-dependent norm

$$||\boldsymbol{v}||_{n+\theta} = \left(\sum_{j=1}^{N}(v_j)^2[\theta h_j^{n+1} + (1-\theta)h_j^n]\right)^{\frac{1}{2}},$$

which is induced by the inner product

$$\langle \boldsymbol{v}, \boldsymbol{w}\rangle_{n+\theta} = \sum_{j=1}^{N-1}[\theta h_j^{n+1} + (1-\theta)h_j^n]v_j w_j\,.$$

For this $\theta$-method we have the following stability theorem.

**Theorem 5.2** *The discrete solution obtained using the $\theta$-method with*

$$\theta = \frac{\rho^{n+1}}{\rho^{n+1} + \rho^n} \,,$$

*satisfies the following a priori bound*

$$||\boldsymbol{c}^{n+1}||^2_{n+1} \leq ||\boldsymbol{c}^n||^2_n - 2\kappa\Delta t \, ||\theta D_+ \boldsymbol{c}^{n+1} + (1-\theta) D_+ \boldsymbol{c}^n||^2_{n+\theta} \,, \tag{5.6}$$

*and hence the method is unconditionally stable.*

**Proof** Multiplying throughout the $\theta$-method by $\theta c_j^{n+1} + (1-\theta)c_j^n$ we obtain

$$\theta^2(\overline{BE})c_j^{n+1} + \theta(1-\theta)(\overline{BE})c_j^n + \theta(1-\theta)(\overline{FE})c_j^{n+1} + (1-\theta)^2(\overline{FE})c_j^n \,, \tag{5.7}$$

where $\overline{BE}$ and $\overline{FE}$ denote the modified BE and FE schemes. To evaluate $\sum_{j=1}^{N-1}(5.7)$ we need to first evaluate $\sum_{j=1}^{N-1}(\overline{BE})c_j^n$ and $\sum_{j=1}^{N-1}(\overline{FE})c_j^{n+1}$. If we multiply (5.4) by $c_j^n$ and sum over interior nodes we obtain

$$\sum_{j=1}^{N-1} \rho^{n+1}(1+\gamma\Delta t)c_j^{n+1}c_j^n = \sum_{j=1}^{N-1} \rho_j^n (c_j^n)^2 + \kappa\frac{\Delta t}{\Delta\xi}\sum_{j=1}^{N-1}\left\{\frac{c_{j+1}^{n+1} - c_j^{n+1}}{h_{j+1}^\theta} - \frac{c_j^{n+1} - c_{j-1}^{n+1}}{h_j^\theta}\right\} c_j^n. \tag{5.8}$$

Replacing the term $c_j^{n+1}c_j^n$ using (5.2) and substituting for $\rho^{n+1}$ in the resulting expression gives

$$\begin{aligned}(1+2\gamma\Delta t)||\boldsymbol{c}^{n+1}||^2_{n+1} &= ||\boldsymbol{c}^n||^2_n + ||\boldsymbol{c}^{n+1} - \boldsymbol{c}^n||^2_{n+1} - \Delta\xi\sum_{j=1}^{N-1}[\rho^{n+1} - \rho^n](c_j^{n+1})^2 \\ &\quad + 2\kappa\frac{\Delta t}{\Delta\xi}\sum_{j=1}^{N-1}\left\{\frac{c_{j+1}^n - c_j^n}{h_{j+1}^\theta} - \frac{c_j^n - c_{j-1}^n}{h_j^\theta}\right\} c_j^n. \end{aligned} \tag{5.9}$$

For $\sum_{j=1}^{N-1}(\overline{FE})c_j^{n+1}$, we have

$$\begin{aligned}||\boldsymbol{c}^{n+1}||^2_{n+1} &= (1-2\gamma\Delta t)||\boldsymbol{c}^n||^2_n - ||\boldsymbol{c}^{n+1} - \boldsymbol{c}^n||^2_n - \Delta\xi\sum_{j=1}^{N-1}[\rho^{n+1} - \rho^n](c_j^n)^2 \\ &\quad + 2\kappa\frac{\Delta t}{\Delta\xi}\sum_{j=1}^{N-1}\left\{\frac{c_{j+1}^n - c_j^n}{h_{j+1}^\theta} - \frac{c_j^n - c_{j-1}^n}{h_j^\theta}\right\} c_j^{n+1}. \end{aligned} \tag{5.10}$$

We now have: $\sum_{j=1}^{N-1}(\overline{BE})c_j^{n+1}$ using (5.1) with $h_j^{n+1}$ replaced by $h_j^\theta$ in the diffusive term and after multiplying by $2\Delta\xi$ gives

$$(1+2\gamma\Delta t)||\boldsymbol{c}^{n+1}||^2_{n+1} = ||\boldsymbol{c}^n||^2_n - ||\boldsymbol{c}^{n+1} - \boldsymbol{c}^n||^2_n - 2\kappa\Delta t||D_+\boldsymbol{c}^{n+1}||^2_{n+\theta} - \Delta\xi\sum_{j=1}^{N-1}[\rho^{n+1} - \rho^n](c_j^{n+1})^2.$$

Calculating $\sum_{j=1}^{N-1}(\overline{FE})c_j^n$ using (5.2) with $h_j^n$ replaced by $h_j^\theta$ in the diffusive term after multiplication by $2\Delta\xi$ gives

$$||\boldsymbol{c}^{n+1}||_{n+1}^2 = (1-2\gamma\Delta t)||\boldsymbol{c}^n||_n^2 + ||\boldsymbol{c}^{n+1}-\boldsymbol{c}^n||_n^2 - 2\kappa\Delta t||D_+\boldsymbol{c}^n||_{n+\theta}^2 - \Delta\xi\sum_{j=1}^{N-1}[\rho^{n+1}-\rho^n](c_j^n)^2.$$

Using (5.9), (5.10) and the previous two equations in $\sum_{j=1}^{N-1}(5.7)$, we now have

$$\begin{aligned}(1+2\theta\gamma\Delta t)||\boldsymbol{c}^{n+1}||_{n+1}^2 &= (1-2(1-\theta)\gamma\Delta t)||\boldsymbol{c}^n||_n^2 - \theta||\boldsymbol{c}^{n+1}-\boldsymbol{c}^n||_n^2 + (1-\theta)||\boldsymbol{c}^{n+1}-\boldsymbol{c}^n||_{n+1}^2 \\ &\quad -2\theta^2\kappa\Delta t\,||D_+\boldsymbol{c}^{n+1}||_{n+\theta}^2 - 2(1-\theta)^2\kappa\Delta t\,||D_+\boldsymbol{c}^n||_{n+\theta}^2 \\ &\quad -\Delta\xi\sum_{j=1}^{N-1}[\rho^{n+1}-\rho^n]\big(\theta(c_j^{n+1})^2+(1-\theta)(c_j^n)^2\big) + \mathrm{I},\end{aligned}$$

where

$$\begin{aligned}\mathrm{I} &= 2\kappa\theta(1-\theta)\Delta t\sum_{j=1}^{N-1}\left\{\left(\frac{c_{j+1}^{n+1}-c_j^{n+1}}{h_{j+1}^\theta}-\frac{c_j^{n+1}-c_{j-1}^{n+1}}{h_j^\theta}\right)c_j^n\right. \\ &\qquad \left.+\left(\frac{c_{j+1}^n-c_j^n}{h_{j+1}^\theta}-\frac{c_j^n-c_{j-1}^n}{h_j^\theta}\right)c_j^{n+1}\right\}.\end{aligned}$$

On simplification of I, we obtain

$$\begin{aligned}\mathrm{I} &= -4\kappa\theta(1-\theta)\Delta t\sum_{j=0}^{N-1}\left(\frac{c_{j+1}^{n+1}-c_j^{n+1}}{h_{j+1}^\theta}\right)\left(\frac{c_{j+1}^n-c_j^n}{h_{j+1}^\theta}\right)h_{j+1}^\theta \\ &= -4\kappa\theta(1-\theta)\Delta t\langle D_+\boldsymbol{c}^{n+1}, D_+\boldsymbol{c}^n\rangle_{n+\theta}\,.\end{aligned}$$

Hence, we have

$$\begin{aligned}||\boldsymbol{c}^{n+1}||_{n+1}^2 &\le ||\boldsymbol{c}^n||_n^2 - 2\kappa\Delta t||\theta D_+\boldsymbol{c}^{n+1}+(1-\theta)D_+\boldsymbol{c}^n||_{n+\theta}^2 \\ &\quad -\theta||\boldsymbol{c}^{n+1}-\boldsymbol{c}^n||_n^2 + (1-\theta)||\boldsymbol{c}^{n+1}-\boldsymbol{c}^n||_{n+1}^2. \qquad (5.11)\end{aligned}$$

We can see from (5.11) that the method will be unconditionally stable and (5.6) will hold if we can ensure that

$$\sum_{j=1}^{N-1}[-\theta\rho^n+(1-\theta)\rho^{n+1}](c_j^{n+1}-c_j^n)^2 \le 0.$$

A sufficient condition that ensures that this inequality holds is to choose

$$\theta = \frac{\rho^{n+1}}{\rho^{n+1} + \rho^n},$$

and this completes the proof. □

**Remark 3** *If the domain is growing, then* $\rho^{n+1} > \rho^n$ *and hence* $1/2 < \theta < 1$. *One might imagine that the above analysis is unduly pessimistic and that the conservative CN scheme, which corresponds to the choice of* $\theta = 1/2$, *is unconditionally stable. However, numerical experiments in Section 7 show that the conservative CN scheme is not unconditionally stable.*

**Remark 4** *If* $\rho(t)$ *is smooth in the sense that* $|\rho_{tt}| < C$ *for* $t \in [0, T]$ *where* $C$ *is a bounded constant, then using Taylor expansions it is relatively simple to show that* $\theta = 1/2 + O(\Delta t)$.

# 6 Convergence result

In this section, we establish a convergence result for the $\theta$-method applied to the conservative formulation. The following lemma establishes a bound on the truncation error.

**Lemma 6.1** *If the* $\theta$*-method is applied to the solution of (3.2), then the truncation error satisfies the bound*

$$T_j^{n+1} = \frac{\gamma(1-2\theta)\Delta t}{2}(\dot{\rho c}) + \frac{\kappa(1-2\theta)\Delta t}{2\rho}\left(\dot{c}_{\xi\xi} + \frac{c_{\xi\xi}}{\rho}\right) + O(\Delta t)^2 + O(N^{-2}),$$

*where all derivatives are evaluated at* $(x_j^{n+1/2}, t_{n+1/2})$.

**Proof** If the domain growth is uniform, then $x_\xi(t) = \rho(t)$ and the exact solution satisfies the conservative formulation

$$(\dot{\rho c}) - \frac{\kappa}{\rho} c_{\xi\xi} + \rho\gamma c = 0.$$

The numerical approximation satisfies the equation

$$\begin{aligned}\frac{\rho^{n+1}c_j^{n+1}-\rho^n c_j^n}{\Delta t} &= \theta L_j^{n+1}c_j^{n+1}+(1-\theta)L_j^n c_j^n \qquad (6.1)\\ &= \frac{\theta\kappa}{\rho^{n+1}}\frac{(c_{j+1}^{n+1}-2c_j^{n+1}+c_{j-1}^{n+1})}{(\Delta\xi)^2}-\theta\rho^{n+1}\gamma c_j^{n+1}\\ &\quad+\frac{(1-\theta)\kappa}{\rho^n}\frac{(c_{j+1}^{n}-2c_j^{n}+c_{j-1}^{n})}{(\Delta\xi)^2}-(1-\theta)\rho^n\gamma c_j^n\ . \qquad (6.2)\end{aligned}$$

We define the truncation error as

$$\begin{aligned}T_j^{n+1} &= \frac{\rho^{n+1}c(x_j^{n+1},t_{n+1})-\rho^n c(x_j^n,t_n)}{\Delta t}-\theta L_j^{n+1}c(x_j^{n+1},t_{n+1})-(1-\theta)L_j^n c(x_j^n,t_n) \qquad (6.3)\\ &= \frac{\rho^{n+1}c(x_j^{n+1},t_{n+1})-\rho^n c(x_j^n,t_n)}{\Delta t}-\frac{\theta\kappa}{\rho^{n+1}}\frac{\Big(c(x_{j+1}^{n+1},t_{n+1})-2c(x_j^{n+1},t_{n+1})+c(x_{j-1}^{n+1},t_{n+1})\Big)}{(\Delta\xi)^2}\\ &\quad+\theta\rho^{n+1}\gamma c(x_j^{n+1},t_{n+1})+(1-\theta)\rho^n\gamma c(x_j^n,t_n)\\ &\quad-\frac{\theta\kappa}{\rho^n}\frac{\Big(c(x_{j+1}^{n},t_{n})-2c(x_j^{n},t_{n})+c(x_{j-1}^{n},t_{n})\Big)}{(\Delta\xi)^2}. \qquad (6.4)\end{aligned}$$

To simplify the truncation error we use the Taylor expansions

$$\rho^n=\rho^{n+1/2}-\frac{\Delta t}{2}\rho_t^{n+1/2}+\frac{(\Delta t)^2}{8}\rho_{tt}^{n+1/2}+O(\Delta t)^3,$$

$$c(x_j^n,t_n)=c(x_j^{n+1/2},t_{n+1/2})-\frac{\Delta t}{2}\dot{c}^{n+1/2}+\frac{(\Delta t)^2}{8}\ddot{c}^{n+1/2}+O(\Delta t)^3,$$

and similar expansions for $\rho^{n+1}$ and $c(x_j^{n+1},t_{n+1})$. Therefore,

$$\frac{\rho^{n+1}c(x_j^{n+1},t_{n+1})-\rho^n c(x_j^n,t_n)}{\Delta t}=\Big(\rho^{n+1/2}\dot{c(x_j^{n+1/2}},t_{n+1/2})\Big)+O(\Delta t)^2\ .$$

It is easy to show that

$$\frac{\Big(c(x_{j+1}^{n+1},t_{n+1})-2c(x_j^{n+1},t_{n+1})+c(x_{j-1}^{n+1},t_{n+1})\Big)}{(\Delta\xi)^2}=c_{\xi\xi}+\frac{(\Delta\xi)^2}{12}c_{\xi\xi\xi\xi}+O(\Delta\xi)^4,$$

where the derivatives are evaluated at $(x_j^{n+1},t_{n+1})$. Hence, overall we have

$$T_j^{n+1}=\frac{\gamma(1-2\theta)\Delta t}{2}\dot{(\rho c)}+\frac{\kappa(1-2\theta)\Delta t}{2\rho}\left(\dot{c}_{\xi\xi}+\frac{c_{\xi\xi}}{\rho}\right)+O(\Delta t)^2+O(N^{-2}),$$

where all derivatives are evaluated at $(x_j^{n+1/2},t_{n+1/2})$. □

We now derive a bound on the global error.

**Theorem 6.1** *If the θ-method is applied to the solution of (3.2), then the global error satisfies the bound*

$$||\boldsymbol{E}^{n+1}||_{n+1} \leq 2\Delta t \sum_{i=1}^{n+1} ||\tilde{\boldsymbol{T}}^{i}||_{i} \ ,$$

*where* $\tilde{T}_j^n = T_j^n/\rho^n$, $j = 1, \ldots, N-1$.

**Proof** Define the local solution $\hat{c}_j^{n+1}$ and the local error $\hat{T}_j^{n+1}$ as follows

$$\frac{\rho^{n+1}\hat{c}_j^{n+1} - \rho^n c(x_j^n, t_n)}{\Delta t} = \theta L_j^{n+1}\hat{c}_j^{n+1} + (1-\theta)L_j^n c_j^n \ , \tag{6.5}$$

$$\hat{T}_j^{n+1} = \hat{c}_j^{n+1} - c(x_j^{n+1}, t_{n+1}) \ . \tag{6.6}$$

Since

$$E_j^{n+1} = c_j^{n+1} - \hat{c}_j^{n+1} + \hat{c}_j^{n+1} - c(x_j^{n+1}, t_{n+1}),$$

we have

$$||\boldsymbol{E}^{n+1}||_{n+1} \leq ||\boldsymbol{c}^{n+1} - \hat{\boldsymbol{c}}^{n+1}||_{n+1} + ||\hat{\boldsymbol{c}}^{n+1} - \boldsymbol{c}(x^{n+1}, t_{n+1})||_{n+1} \ . \tag{6.7}$$

Subtracting (6.5) from (6.1) we obtain

$$\rho^{n+1}[c_j^{n+1} - \hat{c}_j^{n+1}] - \rho^n[c_j^n - \hat{c}_j^n] = \Delta t\Big(\theta L_j^{n+1}(c_j^{n+1} - \hat{c}_j^{n+1}) + (1-\theta)L_j^n(c_j^n - \hat{c}_j^n)\Big) \ ,$$

since $\hat{c}_j^n = c(x_j^n, t_n)$. Using the stability result (5.6), we have

$$||\boldsymbol{c}^{n+1} - \hat{\boldsymbol{c}}^{n+1}||_{n+1} \leq ||\boldsymbol{c}^n - \hat{\boldsymbol{c}}^n||_n = ||\boldsymbol{E}^n||_n \ .$$

Therefore, (6.7) may be rewritten as

$$\begin{aligned} ||\boldsymbol{E}^{n+1}||_{n+1} &\leq ||\boldsymbol{E}^n||_n + ||\hat{\boldsymbol{c}}^{n+1} - \boldsymbol{c}(x^{n+1}, t_{n+1})||_{n+1} \\ &= ||\boldsymbol{E}^n||_n + ||\hat{\boldsymbol{T}}^{n+1}||_{n+1} \ . \end{aligned} \tag{6.8}$$

From equation (6.6), using (6.3) and (6.5), we have

$$\begin{aligned} \rho^{n+1}\hat{T}_j^{n+1} &= \rho^{n+1}\hat{c}_j^{n+1} - \rho^{n+1}c(x_j^{n+1}, t_{n+1}) \\ &= -\left[\rho^{n+1}c(x_j^{n+1}, t_{n+1}) - \rho^n c(x_j^n, t_n)\right] + \Delta t(\theta L_j^{n+1}\hat{c}^{n+1} + (1-\theta)L_j^n\hat{c}^n) \\ &= -\Delta t T_j^{n+1} + \Delta t(\theta L_j^{n+1}\hat{c}_j^{n+1} + (1-\theta)L_j^n\hat{c}_j^n), \end{aligned}$$

so that

$$\rho^{n+1}\hat{T}_j^{n+1} = -\Delta t T_j^{n+1} + \Delta t(\theta L_j^{n+1}\hat{T}_j^{n+1} + (1-\theta)L_j^n\hat{T}_j^n) \ . \tag{6.9}$$

Noting that $\hat{T}_j^n = 0$, we may rewrite (6.9) as

$$\frac{\rho^{n+1}\hat{T}_j^{n+1} - \rho^n\hat{T}_j^n}{\Delta t} = \theta L_j^{n+1}\hat{T}_j^{n+1} + (1-\theta)L_j^n\hat{T}_j^n - T_j^{n+1}.$$

Therefore, except for the truncation error term, we see that $\hat{T}_j^{n+1}$ satisfies the same equation as the numerical solution. Therefore, proceeding in the same way as the proof of Theorem 5.2, we get

$$||\hat{\boldsymbol{T}}^{n+1}||_{n+1}^2 \leq 2\Delta t \left| \sum_{j=1}^{N-1} \rho^{n+1}\hat{T}_j^{n+1}(T_j^{n+1}/\rho^{n+1}) \right| \ ,$$

and hence using Cauchy-Schwartz

$$||\hat{\boldsymbol{T}}^{n+1}||_{n+1} \leq 2\Delta t||\tilde{\boldsymbol{T}}^{n+1}||_{n+1} \ .$$

The equation for the global error (6.8) now takes the form

$$||\boldsymbol{E}^{n+1}||_{n+1} \leq ||\boldsymbol{E}^n||_n + 2\Delta t||\tilde{\boldsymbol{T}}^{n+1}||_{n+1} \ ,$$

and hence we have

$$||\boldsymbol{E}^{n+1}||_{n+1} \leq 2\Delta t \sum_{i=1}^{n+1} ||\tilde{\boldsymbol{T}}^i||_i \ .$$

□

**Remark 5** *Theorem 6.1 establishes that the global error is bounded by $\tilde{T}_j^n = T_j^n/\rho^n$ and hence the global error converges at the rate $O(\Delta t)^2 + O(N^{-2})$ if $\theta = 1/2 + O(\Delta t)$, which will be guaranteed if the growth function $\rho(t)$ is sufficiently smooth as discussed in Remark 4.*

# 7 Numerical experiments

## 7.1 Exponential growth

Figure 2 shows the behaviour of $||\boldsymbol{c}^n||_n$ using the five methods considered in this paper. The calculations were performed assuming uniform exponential growth so that $\rho(t) = e^{St}$ with the parameters $\gamma = 1$, $\kappa = 1$, $S = 0.5$ and in (a) $\Delta t = 1$ and in (b) $\Delta t = 0.1$. From Fig. 2(a) we see that when the time step is relatively large there is an unphysical initial increase in the $L_2$ norm of the solution using both conservative and non-conservative formulations of the Crank-Nicolson scheme. On the other hand, the other three methods all exhibit the correct qualitative behaviour of monotonic decrease in the $L_2$ norm. When we reduce the time step we find that all the solutions decrease monotonically. As expected however, the accuracy of the backward Euler schemes are poor in comparison with the three second-order methods. Note that the best accuracy is obtained using the adaptive $\theta$-method. When $\rho(t) = e^{St}$ the parameter $\theta = e^{S\Delta t}/(e^{S\Delta t} + 1)$ and hence $\theta$ is constant if a uniform time step is used.

## 7.2 Logistic growth

We next consider the logistic growth function

$$\rho(t) = \frac{e^{St}}{1 + \frac{1}{L}\left(e^{St} - 1\right)},$$

where $S > 0$ and $L > 1$. Note that $\rho(0) = 1$ and $\rho(t) \to L$ as $t \to \infty$. In this case we find that growth is initially approximately exponential before finally saturating. In a phenomenological sense this growth function is more biologically reasonable compared to purely exponential growth. In Figure 3 (a) and (b) we see the computed norms of solutions obtained using the five methods presented earlier using a time step $\Delta t = 1$. We can see that the only methods to predict the correct qualitative behaviour of monotonic decrease in the solution norm are the two BE schemes and the

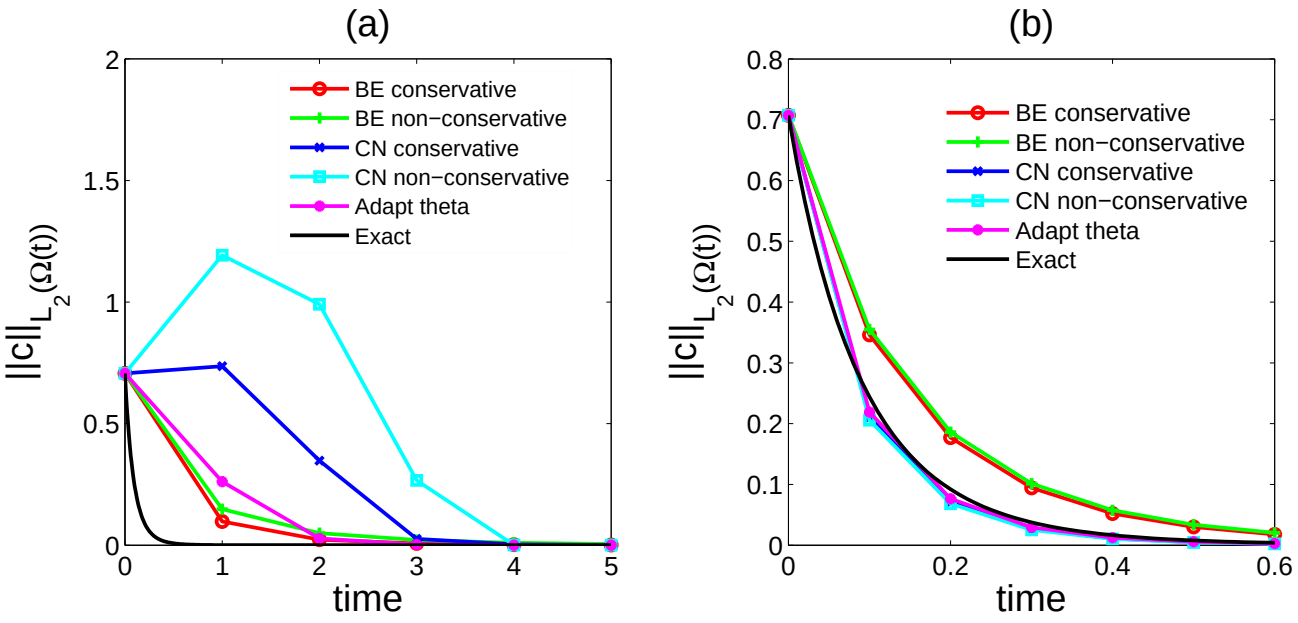


Figure 2: Evolution of $||\boldsymbol{c}^n||_n$ for linear reaction-diffusion problem on an exponentially growing domain: (a) $S = 0.5$, $\gamma = 1$, $\kappa = 1$, $\Delta t = 1$, $\theta = 0.6225$ and (b) $S = 0.5$, $\gamma = 1$, $\kappa = 1$ and $\Delta t = 0.1$, $\theta = 0.5125$.

adaptive $\theta$-method. For logistic growth we find that the parameter $\theta$ is time dependent. Initially, in the exponential growth phase, we see that a relatively large value of $\theta$ has been automatically chosen. As the domain growth slows down and the growth function saturates we see that the value of $\theta \to 1/2$. The simulation was repeated using a smaller value of $\Delta t = 0.1$ and this time we find that all methods exhibit the correct qualitative behaviour. However, we can see clearly that the conservative methods out-perform their non-conservative counterparts and the most accurate approximation is obtained using the adaptive $\theta$-method. Note that the adaptive $\theta$-method chooses automatically a value closer to $1/2$ in-line with the expected $\theta = 1/2 + O(\Delta t)$ behaviour of $\theta$ when the growth function $\rho(t)$ is smooth.

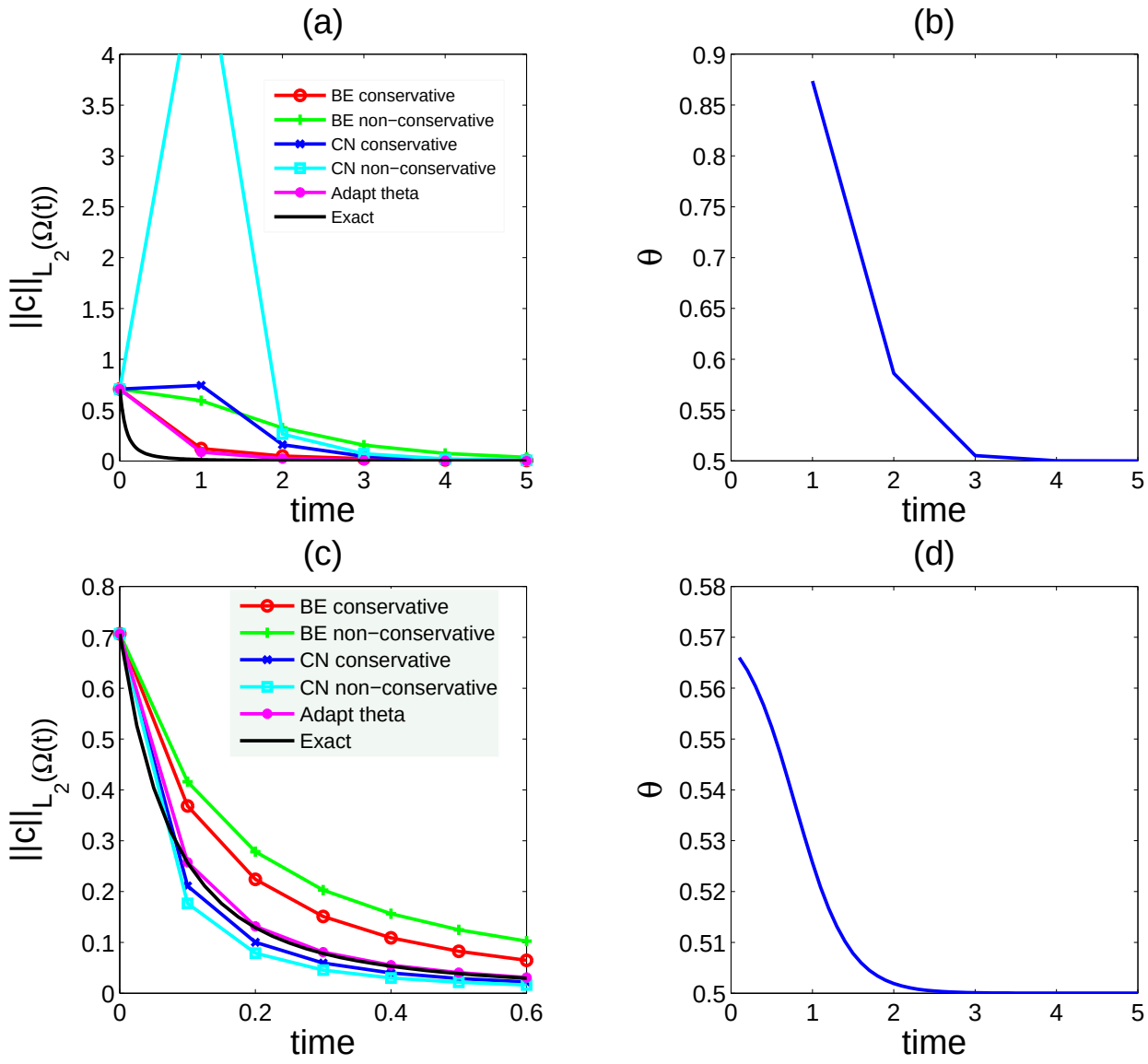


Figure 3: Evolution of $||\boldsymbol{c}^n||_n$ and time integration parameter $\theta$ for linear reaction-diffusion problem on a logistically growing domain with $S = 3$, $\gamma = 1$, $\kappa = 1$, $L = 10$. (a)-(b) $\Delta t = 1$ and (c)-(d) $\Delta t = 0.1$.

# 8 Conclusions

In this paper we have analysed the stability properties of some well known finite difference approximations of a model reaction-diffusion problem on a growing domain. We considered two reformulations of the governing equation which enabled the discretisation to be carried out on a fixed computational domain. Although both formulations are equivalent at the continuous level,

we found that implicit discretisations of the conservative formulation are more stable in the sense that the $L_2$ norm of the solution decreased independently of the choice of the time step and the rate of growth of the domain. By contrast, implicit discretisations of the non-conservative reformulation were generally only conditionally stable, with the maximal allowable time step being related to the rate of domain growth. The biological implications of our findings are that when the domain grows at a rate much faster than the reaction kinetics, then conservative formulations should be used. In particular, the proposed adaptive $\theta$-method provides computational modellers with an efficient, robust and more accurate scheme which is unconditionally stable as opposed to the conditionally stable forward Euler method which is frequently used in biological simulations of most reaction-convection-diffusion systems.

Although the presented analysis is limited to uniform growth of the domain, we expect the stability results to be equally valid for problems where non-uniform domain growth is more appropriate [4]. The methods developed in this paper can also be used for reaction-diffusion problems on contracting domains. Initial analysis and numerical experimentation suggests that discretisations of the conservative formulation are again more stable than non-conservative discretsations and we plan to report these finding elsewhere. Although we have presented results for linear reaction kinetics, our adaptive theta method is also applicable to nonlinear reaction kinetics. However, the stability analysis for such systems is the subject of our current studies. Furthermore, from a biological point of view, no patterns emerge for linear kinetics and hence the need to study nonlinear reaction kinetics. We also plan to extend the analysis to higher dimensional problems and to problems posed on surfaces using the ALE formulation. Most biologically relevant problems are posed on non-rectangular domains so for that reason we will concentrate on finite element discretisations. The analysis presented in [12] would suggest that the satisfaction of a discrete geometric conservation by the time integration scheme will be important to maintain stability.

# References

[1] D. Boffi and L. Gastaldi. Stability and geometric conservation laws for ALE formulations. *Comp. Meth. Appl. Mech. Eng.*, 193:4717–4739, 2004.

[2] V. Castets, E. Dulos, J. Boissonade, and P. De Kepper. Experimental evidence of a sustained standing Turing-type nonequilibrium chemical pattern. *Phys. Rev. Lett.*, 64:2953–2956, 1990.

[3] E.J. Crampin, E.A. Gaffney, and P.K. Maini. Reaction and diffusion on growing domains: Scenarios for robust pattern formation. *Bull. Math. Biol.*, 61:1093–1120, 1999.

[4] E.J. Crampin, W.W. Hackborn, and P.K. Maini. Pattern formation in reaction-diffusion models with non-uniform domain growth. *Bull. Math. Biol.*, 64:746–769, 2002.

[5] J. Donea, S.Giuliani, and J.P. Halleux. An Arbitrary Lagrangian-Eulerian finite element method for transient dynamic fluid-structure interactions. *Comp. Meth. Appl. Mech. Engrg.*, 33:689–723, 1982.

[6] L. Formaggia and F. Nobile. A stability analysis for the arbitrary Lagrangian Eulerian formulation with finite elements. *East-West Journal of Numerical Mathematics*, 7:105–131, 1999.

[7] L. Formaggia and F. Nobile. Stability analysis of second-order time accurate schemes for ALE-FEM. *Comp. Meth. Appl. Mech. Eng.*, 193:4097–4116, 2004.

[8] T.J.R. Hughes, W.K. Liu, and T.K. Zimmermann. Lagrangian-Eulerian finite element formulation for incompressible viscous flows. *Comp. Meth. Appl. Mech. Engrg.*, 29:329–349, 1981.

[9] S. Kondo and R. Asai. A reaction-diffusion wave on the skin of the marine angelfish *P*omacanthus. *Nature*, 376:765–768, 1995.

[10] M. Lesoinne and C. Farhat. Geometric conservation laws for flow problems with moving boundaries and deformable meshes, and their impact on aeroelastic computations. *Comput. Methods Appl. Mech. Engrg.*, 134:71–90., 1996.

[11] J.A. Mackenzie and W.R. Mekwi. An analysis of stability and convergence of a finite difference discretisation of a model parabolic PDE in 1D using a moving mesh. *IMA Journal of Numerical Analysis*, 27:507–528, 2007.

[12] J.A. Mackenzie and W.R. Mekwi. An unconditionally stable second-order accurate ALE-FEM scheme for two-dimensional convection-diffusion problems. Technical Report 22, Strathclyde University, Mathematics Department, 2007. Submitted for publication.

[13] A. Madzvamuse. Stability analysis of reaction-diffusion systems with constant coefficients on growing domains. *Int. J. of Dynamical and Differential Equations*, 1(4):250–262, 2008.

[14] A. Madzvamuse and P.K. Maini. Velocity-induced numerical solutions of reaction-diffusion systems on fixed and growing domains. *J. Comput. Phys.*, 225:100–119, 2007.

[15] A. Madzvamuse, P.K. Maini, and A.J. Wathen. A moving grid finite element method applied to a model biological pattern generator. *J. Comput. Phys.*, 190:478–500, 2003.

[16] A. Madzvamuse, P.K. Maini, and A.J. Wathen. A moving grid finite element method for the simulation of pattern generation by Turing models on growing domains. *J. Sci. Comput.*, 24(2):247–262, 2005.

[17] A. Madzvamuse, R.D.K. Thomas, P.K. Maini, and A.J. Wathen. A numerical approach to the study of spatial pattern formation in the Ligaments of Arcoid Bivalves. *Bull. Math. Bio.*, 64:501–530, 2002.

[18] P.K. Maini, R.E. Baker, and C.M. Chong. The Turing model comes of molecular age. *Science*, 314:1397–1398, 2006.

[19] F. Nobile. *Numerical approximation of fluid-structure interaction problems with application to haemodynamics*. PhD thesis, Department of Mathematics, École Polytechnique Fédérale de Lausanne, 2001.

[20] Q. Ouyang and H.L. Swinney. Transition from a uniform state to hexagonal and striped Turing patterns. *Nature*, 352:610–612, 1991.

[21] R. Plaza, F. Sanchez-Garduno, P. Padilla, R.A. Barrio, and P.K. Maini. The effect of growth and curvature on pattern formation. *J. Dyn. Differ. Equ.*, 16(4):1093–1121, 2004.

[22] S. Sick, S. Reinker, J. Timmer, and T. Schalke. WNT and DKK determine hair follicle spacing through a reaction-diffusion mechanism. *Science*, 314:1447–1450, 2006.

[23] L. Solnica-Krezel. Vertebrate development: Taming the nodal waves. *Curr Biol.*, 13:R7–9, 2003.

[24] A.M. Turing. The chemical basis of morphogenesis. *Philos. Trans. R. Soc. London, Ser. B*, 237:37–72, 1952.